Chaos
An Interdisciplinary Journal of Nonlinear Science

Recursive traffic percolation on urban transportation systems

Cite as: Chaos **33**, 033132 (2023); https://doi.org/10.1063/5.0137726
Submitted: 05 December 2022 • Accepted: 01 February 2023 • Published Online: 21 March 2023

Zhuoran Chen, Chao Yang, Jiang-Hai Qian, et al.

COLLECTIONS

Note: This paper is part of the Focus Issue on Disruption of Networks and System Dynamics.

This paper was selected as Featured

View Online Export Citation CrossMark


Chaos
Special Topic: Nonlinear Model Reduction From Equations and Data
Submit Today!

AIP Publishing

© 2023 Author(s).

Recursive traffic percolation on urban transportation systems

Cite as: Chaos 33, 033132 (2023); doi: 10.1063/5.0137726
Submitted: 5 December 2022 · Accepted: 1 February 2023 ·
Published Online: 21 March 2023

View Online Export Citation CrossMark

Zhuoran Chen,[1] Chao Yang,[1] Jiang-Hai Qian,[2,a)] Dingding Han,[1,3,4,a)] and Yu-Gang Ma[4,5,a)]

AFFILIATIONS

[1]School of Information Science and Technology, Fudan University, Shanghai 200433, China
[2]College of Mathematics and Physics, Shanghai University of Electric Power, Shanghai 200090, China
[3]Shanghai Artificial Intelligence Laboratory, Shanghai 200232, China
[4]Shanghai Research Center for Theoretical Nuclear Physics, NSFC and Fudan University, Shanghai 200438, China
[5]Key Laboratory of Nuclear Physics and Ion-Beam Application (MOE), Institute of Modern Physics, Fudan University, Shanghai 200433, China

Note: This paper is part of the Focus Issue on Disruption of Networks and System Dynamics.
[a)]**Authors to whom correspondence should be addressed:** qianjianghai@shiep.edu.cn; ddhan@fudan.edu.cn; mayugang@fudan.edu.cn

ABSTRACT

This paper proposes a recursive traffic percolation framework to capture the dynamics of cascading failures and analyze potential overloaded bottlenecks. In particular, compared to current work, the influence of external flow is considered, providing a new perspective for the study of regional commuting. Finally, we present an empirical study to verify the accuracy and effectiveness of our framework. Further analysis indicates that external flows from different regions affect the network. Our work requires only primary data and verifies the improvement of the functional network.

Published under an exclusive license by AIP Publishing. https://doi.org/10.1063/5.0137726

Traffic percolation has attracted widespread attention in recent years. The transition between isolated local and global flows helps to understand the intrinsic feature of traffic dynamics. For commuting in an open area of a city, it includes both the traffic within its road network and the flow exchange with external areas. Here, we study the cascading failure of traffic percolation in urban transportation systems. We propose a recursive traffic percolation framework to capture the dynamics of cascading failures and analyze the potential overloaded bottlenecks. First, we use population data to generate trips from origins to destinations and consider internal and external flows. Then, we assign trips to the road network via the shortest paths and convert the load on each road segment to velocity based on the car-following model. We repeatedly perform edge removal and load redistribution until no more edges are removed from the functional network. By traversing the percolation threshold, the phase transition of the percolation process occurs where the second-largest giant component reaches its maximum. We define the edges causing this transition as bottlenecks. We show that the proposed percolation framework is helpful in capturing the dynamics of cascading failures and find the network bottlenecks. By improving the volume of identified bottlenecks, the global flow is benefited and the phase transition of percolation is delayed.

I. INTRODUCTION

Urban transportation systems are susceptible to various factors, such as weather, special events, and congestion, resulting in high traffic delays.[1–6] The typical approach to improving urban transportation is to reduce delays under normal conditions. Efforts have been made to improve traffic efficiency by improving road network infrastructure and organizing traffic demands.[7–10] However, studies have found that even minor improvements in bottlenecks can significantly impact global mobility.[11,12]

Percolation theory[13–25] has significantly contributed to describing the structure, functionality, and resilience of transportation systems from the perspective of network science. In traffic percolation (TP),[26–28] intersections in the road network are mapped as nodes, and roads are modeled as edges weighted by traffic indicators,

Published under an exclusive license by AIP Publishing

such as the ratio of instantaneous velocity to the upper-velocity limit. The edge failure of the converted network represents extreme conditions in urban transportation systems, such as congestion. TP simulates edge failure by gradually removing edges from the network as the threshold approaches. The breakdown of the network under edge removal is not a gradual process. Removing a small fraction of edges has only a limited effect on network integrity. The network breaks into disconnected components once the proportion of removed edges reaches a critical threshold. The impact of edge failure is typically measured by the size change of the networks' giant components. When the largest giant component disintegrates, with the second-largest giant component reaching its maximum, the phase transition occurs where global flows are separated into isolated local flows by bottlenecks.

Mining real time series data captures the dynamic characteristics of urban traffic systems and indicates that different bottlenecks accompanied the evolution of the global flow organization at different times of the day.[29] However, it is challenging to measure the evolutionary behavior of the urban transportation system after optimization. How to evaluate the optimization of the system before its operation becomes an essentially issue. On the basis of known topology, TP alone is only an evaluation of the system performance, which is insufficient to verify the bottleneck improvement. The load redistribution due to congestion needs to be considered. If an edge congests, the load on the edge will choose other edges with less latency, resulting in a redistribution of load in the network. The new load may exceed some edges' capacities and then congest these edges, which is called a cascading failure. Consequently, a significant fraction of the network can be shut down.[30–33]

This paper intends to fill the gap and build the connection between TP and load redistribution. To implement a mechanism for load redistribution, we introduce a recursive traffic percolation (RTP) framework that contains trip generation, load assignment, velocity conversion, and edge removal. Edges with velocity ratios below the percolation threshold are considered congested and are removed from the network. The process of load redistribution and edge removal is repeated on the remaining network and finally generates a network that is still functional at this threshold. By traversing the percolation threshold, the phase transition occurs where the second-largest giant strong component reaches its maximum. The edges causing this transition are identified as the bottlenecks. We also consider external traffic into the network in this framework. The actual congestion conditions of the removed edges verify the model's accuracy. An empirical study on the district scale reveals the effectiveness of the model.

The rest of the paper is organized as follows. Section II presents the proposed framework of RTP and the vulnerability metrics. Section III shows the empirical study in Yangpu District, Shanghai. Section IV summarizes the conclusions of this study and proposes some future directions.

II. METHODS

We apply an approach expanded on the model developed in Ref. 34. The framework is shown in Fig. 1. We first generate a directed weighted network using population distribution and road network topology, followed by RTP over the generated network. RTP includes mainly four steps. First, the radiation model generates trips between the origin and destination regions.[35] Second, the trips are assigned to the road network via the shortest paths. Third, the load on each road segment is converted to velocity according to a car-following model. Finally, the edges with velocity ratios below the threshold are considered dysfunctional and removed from the network. These four steps are repeated for a given velocity ratio threshold until no more edges are removed from the functional network.

A. Trip generation

We use the population counts from WorldPop[36] as a proxy for trip numbers, formatted as Geotiff at a resolution of approximately 100 m. We build Voronoi polygons[37] around intersections as shown in Fig. 2(a) and calculate the population of each polygon N_i by counting all pixels whose center is located within the polygon, as

$$N_i = \sum_{t}^{C_t \in S_i} N_t, \tag{1}$$

where N_t is the population of pixel t, C_t is the center of the pixel t, and S_i is the shape of Voronoi polygon i. The Voronoi polygons weighted by population counts are shown in Fig. 2(b).

Gravity models[38–40] describe the inter-regional flow of travelers in urban transportation networks. However, the need for empirical data to fit the parameters makes it unable to predict mobility in regions where systematic data are lacking.[41] Instead, the radiation model is used in this paper. According to the radiation model, the flow of commuters from an origin region o to a destination region d is proportional to the populations of origin region o and destination region d and inversely proportional to the total population within the distance between them. The fraction of commuters f_{od} is

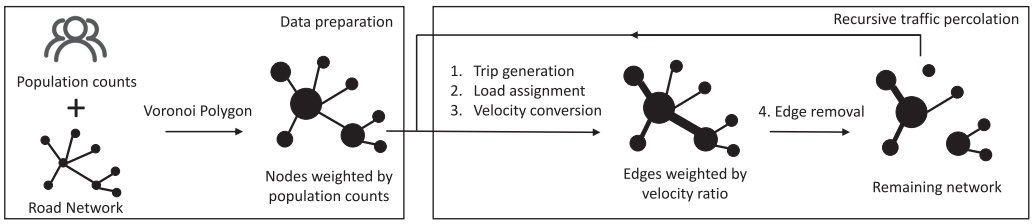

FIG. 1. The framework of the proposed RTP.

Published under an exclusive license by AIP Publishing

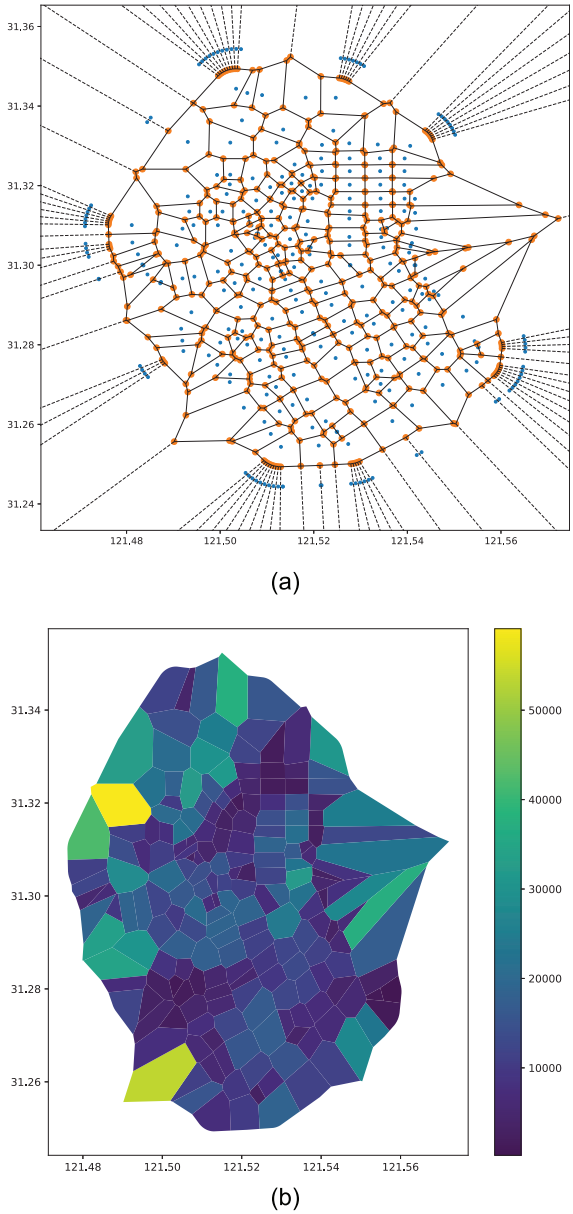

FIG. 2. Voronoi polygons of Observed Yangpu district. (a) The partitioned Voronoi polygons. The orange dots and solid lines represent the vertices and boundaries of the Voronoi polygons, respectively. Blue dots in the polygons represent the intersections while those out of the polygons and dashed lines are used to assist in generating boundary shapes. (b) The Voronoi polygons weighted by population.

defined as

$$f_{od} = \frac{N_o N_d}{(N_o + s_{od})\,(N_o + N_d + s_{od})}, \tag{2}$$

where s_{od} is the total population of the regions within the distance between origin region o and destination region d, excluding the population of destination region N_d. Then, the commuter load L_{od} from origin region o to destination region d is

$$L_{od} = \alpha N_o f_{od}, \tag{3}$$

while α is the proportionality coefficient of commuters to the population of the regions.

The urban area is an open system where, in addition to intra-regional flows, there is also an exchange of flows between external regions. To simulate the influx of flow outside the observed area, we increase the population of bordering regions N_i. The number of external commuters commuting through the polygon that at the verge of the observed area is assumed to be proportional to the polygon's population N_i. Then, the composite population N_i^{bor} compounded by external flow and interior flow is used instead of the original N_i for bordering polygons, as

$$N_i^{bor} = (1 + \beta) N_i, \tag{4}$$

where β is the growth coefficient of the population.

B. Load assignment

Commuters are assumed to optimize their travel time by taking the shortest path. Loads of origin–destination pairs are assumed to be evenly distributed on the roads. The number of commuters on a particular edge e_{ij}, denoted as load L_{ij}, is

$$L_{ij} = l_{ij} \sum_{o,d} \frac{L_{od}}{x_{od}} \theta_{od}(ij), \tag{5}$$

where l_{ij} is the length of edge e_{ij}, x_{od} is the shortest distance of origin region o, and destination region d, $\theta_{od}(ij)$ is a binary variable equal to 0 when the edge e_{ij} is not on the shortest path connecting nodes o and d, and 1 otherwise.

C. Velocity conversion

We use the Daganzo model[42] to derive the velocity from the density of the road segment. Given the edge e_{ij} of length l_{ij} with lane number m_{ij}, let D_{ij} be the density of vehicles per unit length per lane of e_{ij}, then the relationship between L_{ij} and D_{ij} is

$$L_{ij} = l_{ij} m_{ij} D_{ij}. \tag{6}$$

On the other hand, considering the braking distance within reaction time t_r and the vehicle length l_{veh}, the density D_{ij} equals

$$D_{ij} = \frac{1}{l_{veh} + v_{ij} t_r}, \tag{7}$$

where v_{ij} is the converted velocity of e_{ij}, which is limited from the top at the velocity limit V_{ij} set on the edge e_{ij} and limited from the bottom at zero. Then,

$$v_{ij} = \begin{cases} V_{ij}, & D_{ij} \le \frac{1}{l_{veh} + V_{ij} t_r}, \\ \frac{1}{t_r}\left(\frac{1}{D_{ij}} - l_{veh}\right), & \frac{1}{l_{veh} + V_{ij} t_r} < D_{ij} \le \frac{1}{l_{veh}}, \\ 0 & \text{otherwise.} \end{cases} \tag{8}$$

This leads to

$$v_{ij} = \frac{1}{t_r}\left(\frac{m_{ij}}{\sum_{o,d} \frac{L_{od}}{x_{od}} \theta_{od}(ij)} - l_{veh}\right), \quad v_{ij} \in \left[0, V_{ij}\right], \tag{9}$$

where l_{veh} is assumed to be 5 m and t_r is set to 2 s.

Published under an exclusive license by AIP Publishing

D. Edge removal and load redistribution

For each road e_{ij}, r_{ij} is denoted with the ratio between the converted velocity and upper-velocity limit as the traveling capacity measurement, as

$$r_{ij} = \frac{v_{ij}}{V_{ij}}. \tag{10}$$

For a given velocity ratio threshold q, the road e_{ij} can be classified into two categories: functional when $r_{ij} \geq q$ and dysfunctional for $r_{ij} < q$ as

$$e_{ij} = \begin{cases} 1, & r_{ij} \geq q, \\ 0, & r_{ij} < q. \end{cases} \tag{11}$$

Edges with velocity ratios below q are considered dysfunctional and removed from the network. When a node has no connected edges, this node is also removed. After removing edges and nodes, the trips of the remaining nodes are regenerated, and loads of the remaining edges are reassigned. The above process is repeated for the given q value until the functional network no longer changes. The functional network becomes sparser by traversing the threshold of velocity ratio q from 0 to 1, and the RTP is conducted.

E. Vulnerability metrics

A giant component is a subgraph in which any two nodes are connected. The size of the largest giant component reflects the connectivity of complex networks. The second-largest giant component is also used to detect the critical phenomenon in TP. The largest giant strong component coefficient, denoted as G, and the second-largest giant strong component, denoted as SG, are used to measure the functionality of the network, which are formulated as follows:

$$G = \frac{n_{lgc}}{n}, \tag{12}$$

$$SG = \frac{n_{sgc}}{n}, \tag{13}$$

where n_{lgc} and n_{sgc} are the number of nodes contained in the largest giant strong component and second-largest strong component, respectively, and n is the number of nodes in the network.

To observe the dynamics of the functional network, the value of q varies from 0 to 1. A hierarchy of different sizes emerges for a specific value of q, where only clusters of roads with r_{ij} higher than q remain. G and SG are changed with q. When $q = 0$, the network is the same as the original road network; when $q = 1$, it becomes completely fragmented. Critical value q_c is determined as the q value when SG reaches its maximum.

III. EXPERIMENTS

A. Geo-spatial topologies

The empirical study is conducted on the road network of Yangpu District. We establish the road network using data from OpenStreetMap,[43] a knowledge database providing free access to current geographical information. Main roads are extracted by excluding minor roads, residential streets, and service roads, and

FIG. 3. Observed Yangpu District. (a) Road topology. The road topology is formatted as a directed network. (b) Velocity ratio distribution when $\alpha = 30$.

Published under an exclusive license by AIP Publishing

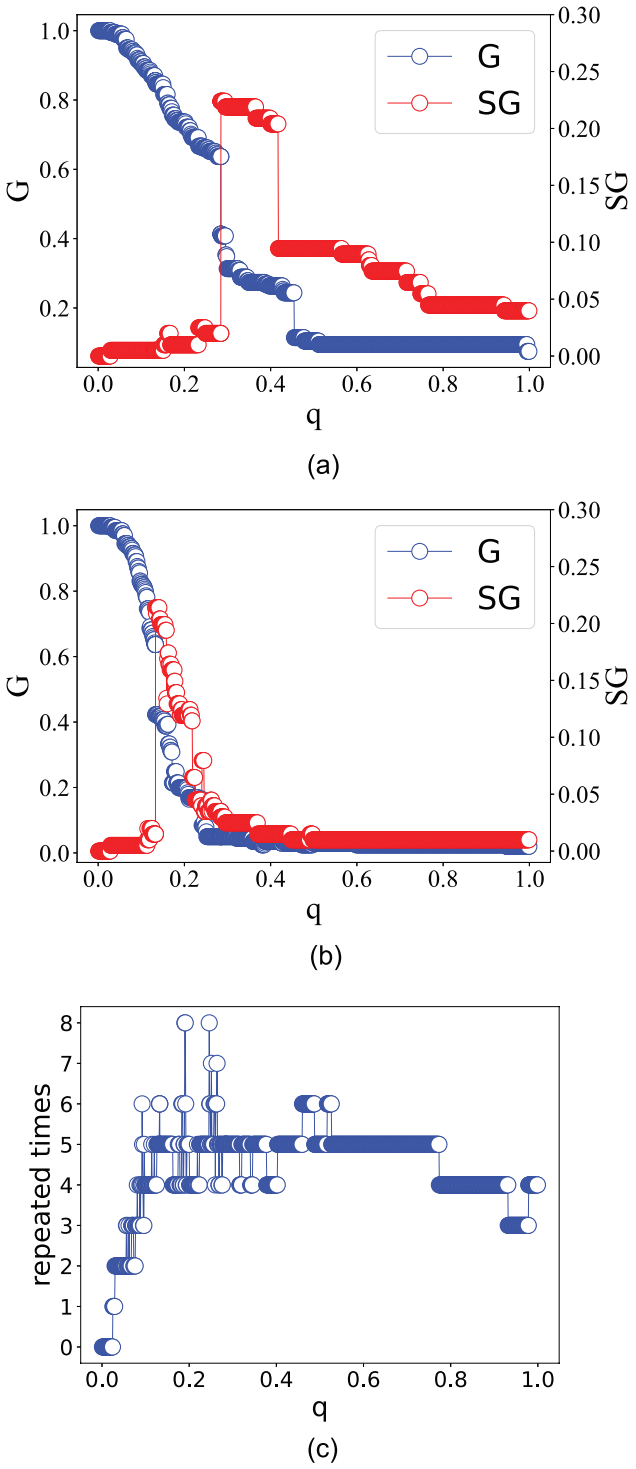

FIG. 4. Results of interior commuting. (a) G and SG of TP. The critical value $q_c^{TP} = 0.2844$. (b) G and SG of RTP. The critical value $q_c^{RTP} = 0.1329$. (c) Repeated times of RTP.

FIG. 5. Origins of external flow: Zhonghuan Road (ZH), Yixian Elevated Road (YX), Guofan Road (GF), Inner Ring Viaduct (IR). When the four regions have external traffic inflow at the same time, it is represented as All.

nodes on the same road are aggregated. The nodes around intersections are consolidated to make clear intersections using OSMnx.[44] Thus, we create the road network in which intersections are represented as nodes and roads are represented as directed edges. The topology of Yangpu District in Shanghai is shown in Fig. 3(a). After trip generation, load assignment and velocity conversion, the velocity ratio distribution is shown in Fig. 3(b).

B. Results of interior commuting

When growth coefficient $\beta = 0$, there is only internal traffic on the network. When velocity ratio threshold q is relatively small, commuters can reach almost any place through the largest giant strong component with a velocity ratio no less than q. However, when q exceeds a certain value, the largest giant strong component with a velocity ratio no less than q will be disconnected, and the global flow will be blocked into local flows.

The results of giant strong component coefficients G and SG changing with velocity ratio threshold q are shown in Figs. 4(a) and 4(b). When proportionality coefficient $\alpha = 30$, the critical value of RTP q_c^{RTP} is 0.1329 while that of TP q_c^{TP} is 0.2844. TP can be

Published under an exclusive license by AIP Publishing

TABLE I. The proportion of real congested edges to the removed edges and the average frequency of removed congested edges.

	TP	RTP	ZH	YX	IR	GF	All
Proportion	0.637	0.610	0.597	0.610	0.607	0.610	0.596
Frequency	4.429	4.844	4.926	4.844	4.800	4.844	4.889

regarded as the first step of RTP, in which all the edges with a velocity ratio below the threshold q are removed. The critical value q_c^{RTP} obtained from the evolution of load redistribution is far less than the critical value q_c^{TP} for only percolation once, which indicates that the load redistribution captures the edges that subsequently suffers cascading failure. The number of repeated times is shown in Fig. 4(c), which increases significantly around the phase transition and then flattens out overall.

The change of the network under TP is monotonous. The larger velocity ratio threshold q is, the higher collapse rate is. In contrast, the results of RTP show fluctuations. When the largest giant strong component starts to collapse rapidly, SG increases to a certain extent compared with the smaller q value, indicating that the sequence of the edges that lost their function is crucial in cascading failure, which leads to different subsequent evolutionary results.

C. Impact of external flow

We select Zhonghuan Road (ZH), Inner Ring Viaduct (IR), Yixian Elevated Road (YX), and Guofan Road (GF) as the traffic influx study regions. As shown in Fig. 5, the observed regions are located on the boundary of Yangpu District and are the main channels connecting with other districts. The populations of these four regions are increased both, respectively, and simultaneously. RTP is used for these five situations.

In order to verify the accuracy of the model, we compare the actual congestion conditions of the removed edges that are considered to be functionally failed. We use the congestion data obtained from Baidu API[45] to verify the congestion conditions of the removed edges. The congestion conditions are sampled multiple times during the morning and evening peaks. The proportion of real congested edges in the removed edges and the average congested frequency of removed congested edges at the critical value q_c are shown in Table I. While TP removes a slightly higher percentage of congested edges, edges removed by RTP have higher congestion levels. There seems to be an inverse relationship between the number of removed edges and the congestion level of the edges, where ZH has the lowest percentage of removed edges but the highest congestion levels, which matches the congestion in the area triggered by an influx of flow in actual traffic conditions.

The relationship between critical threshold q_c and growth coefficient β is shown in Fig. 6. As β increases, the critical value q_c

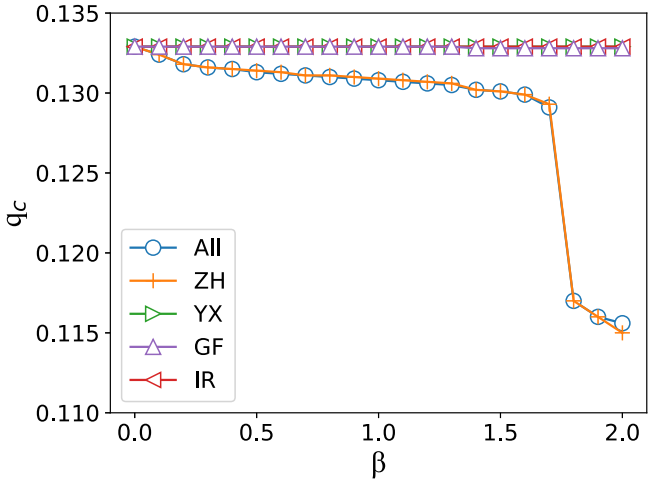

FIG. 6. Effect of external flow on critical value q_c.

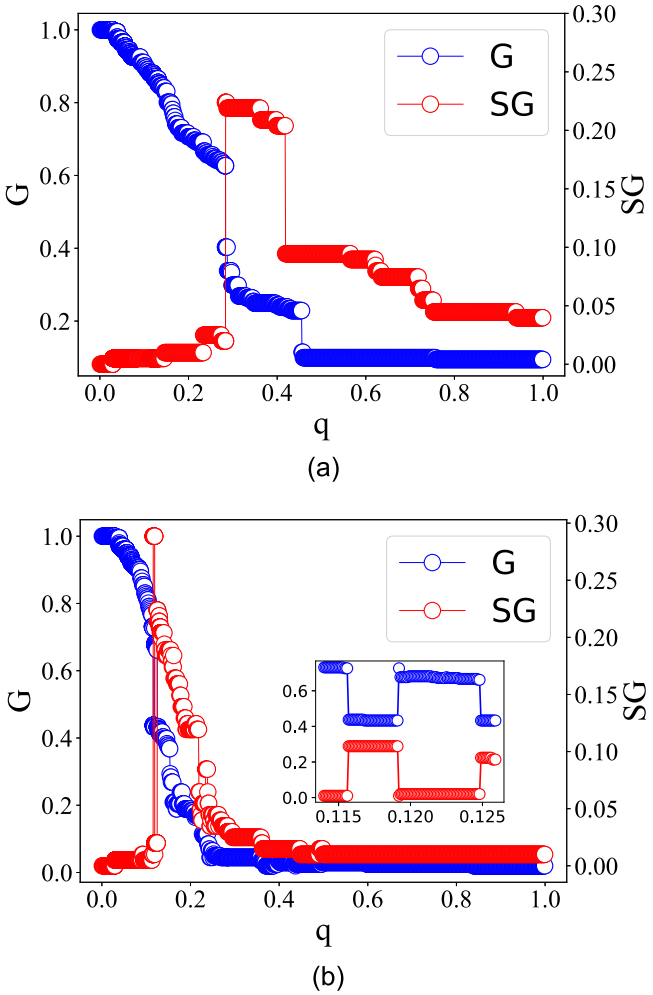

FIG. 7. Impact of the external flow on the network. (a) G and SG of TP. The critical value $q_c^{TP} = 0.2834$. (b) G and SG of RTP. The critical value $q_c^{RTP} = 0.1156$.

Published under an exclusive license by AIP Publishing

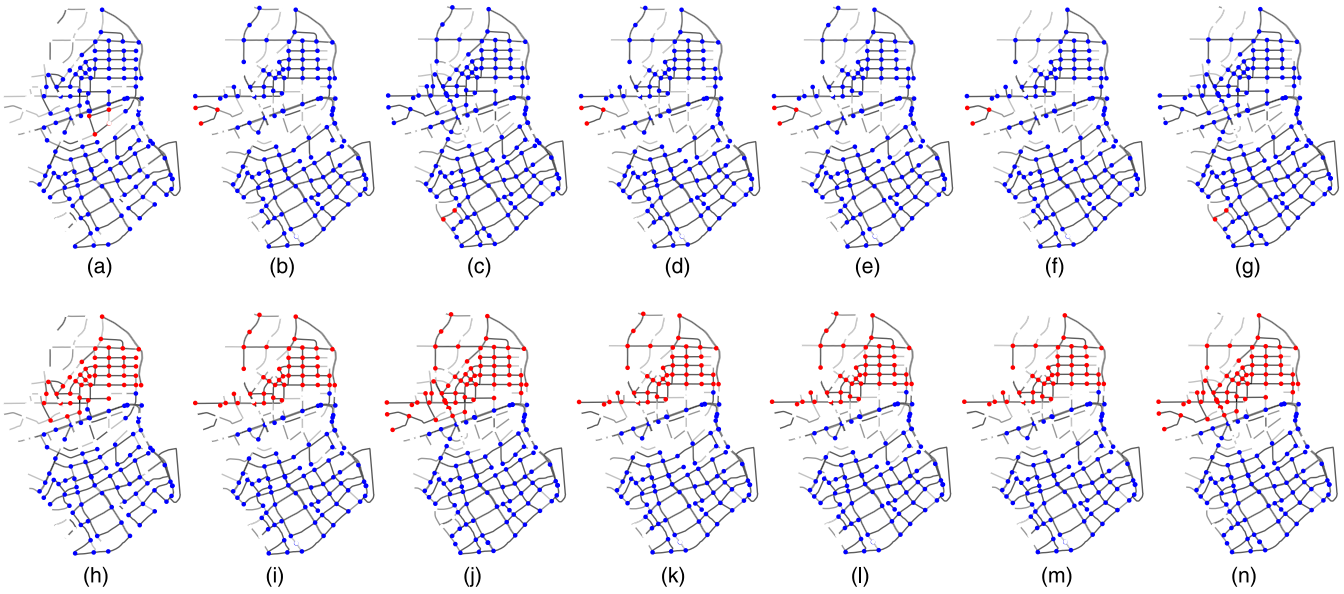

FIG. 8. Remaining nodes (largest giant component in blue and second largest giant component in red) and edges with the external commute. (a)–(g) Before the critical point: (a) TP, (b) RTP, (c) ZH, (d) IR, (e) YX, (f) GF, (g) All; (h)–(n) At the critical point: (h) TP, (i) RTP, (j) ZH, (k) IR, (l) YX, (m) GF, (n) All.

decreases, indicating that the overall connectivity of the network is affected by increasing external flow.

Considering the case where all four regions have an influx of traffic and the growth coefficient $\beta = 2$, the results of G and SG changing with percolation threshold q are shown in Fig. 7. The critical value of RTP q_c^{RTP} is reduced from 0.1329 to 0.1156, while that of TP q_c^{TP} is reduced from 0.2844 to 0.2834. The more significant

FIG. 9. Detection of the bottlenecks. The removed edges are indicated by thick red lines, and the remaining edges are indicated by thin gray lines, where the shades of red vary, with darker color indicating that the edges are broken in both directions and lighter color indicating only one direction is broken. (a) Removed edges before the critical point. (b) Removed edges at the critical point. (c) Bottleneck: Zhongyuan Road from south to north.

Published under an exclusive license by AIP Publishing

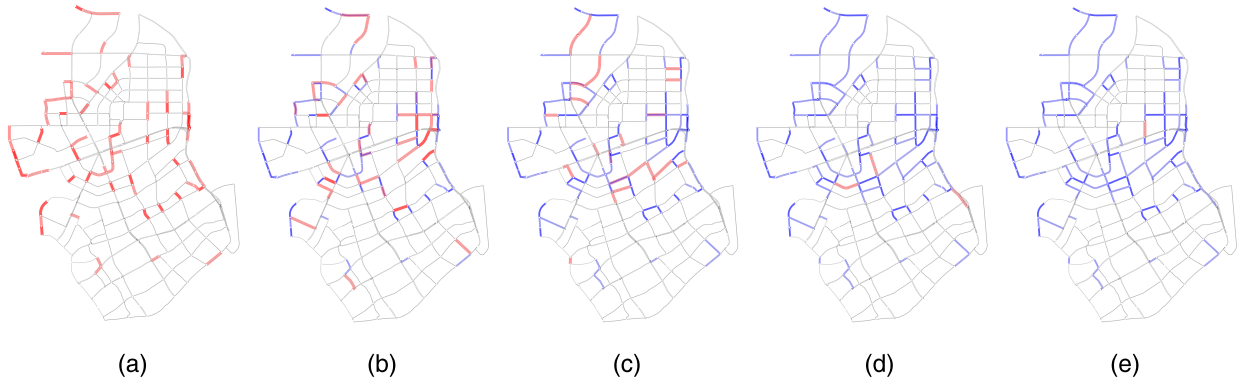

FIG. 10. The cascading edge removals at the critical point. (a)–(e) represent the first to the fifth round edge removal, respectively. The edges removed in the previous rounds and the current round are indicated by blue lines and red lines, respectively.

changes in the critical value of RTP indicate greater sensitivity to changes in dynamic traffic conditions.

The impact of external traffic on the network can be divided into three specific categories. Among the four regions, ZH dominates the influence of external traffic on the network since the overall q_c changes in parallel with that of ZH. As the remaining nodes and edges before and at q_c shown in Fig. 8, the largest giant strong component and the second-largest strong giant component are divided by the ZH. The roads around the IR are more robust and can share the input of external traffic. YX and GF have almost no effect on the network since the roads near these two regions are not connected to the largest giant strong component before critical points, even when external traffic is not considered. As a result, the congestion is generated locally, and the impact on giant components is blocked. It is observed that when β is greater than 1.7, q_c decreases rapidly, and YX is in the largest giant strong component under the current q_c. The external of YX is absorbed by the whole network at this time. The remaining giant components of TP and RTP are also shown in Fig. 8. TP removes more edges than RTP since the critical value of TP q_c^{TP} is much larger than that of RTP q_c^{RTP}, while G and SG are quite similar.

D. Bottleneck detection and improvement

The edges leading to the phase transition where SG reaches its maximum are regarded as the bottlenecks of the functional network. By comparing the edges removed before and at the critical point, the newly removed edges are regarded as bottlenecks, as shown in Fig. 9. The bottleneck obtained is Zhongyuan Road from south to north, which is also one of the congested roads at morning and evening peaks.

The cascading edge removals are studied, as shown in Fig. 10. It is obvious that most of the newly removed edges in this round are adjacent to the removed edges in the previous rounds, and there are also fewer new areas affected by global flow diffusion. It is worth noting that, the bottleneck is found during the fifth round of edge removal. It is through the dynamic process of cascading failure that the hidden bottleneck is discovered.

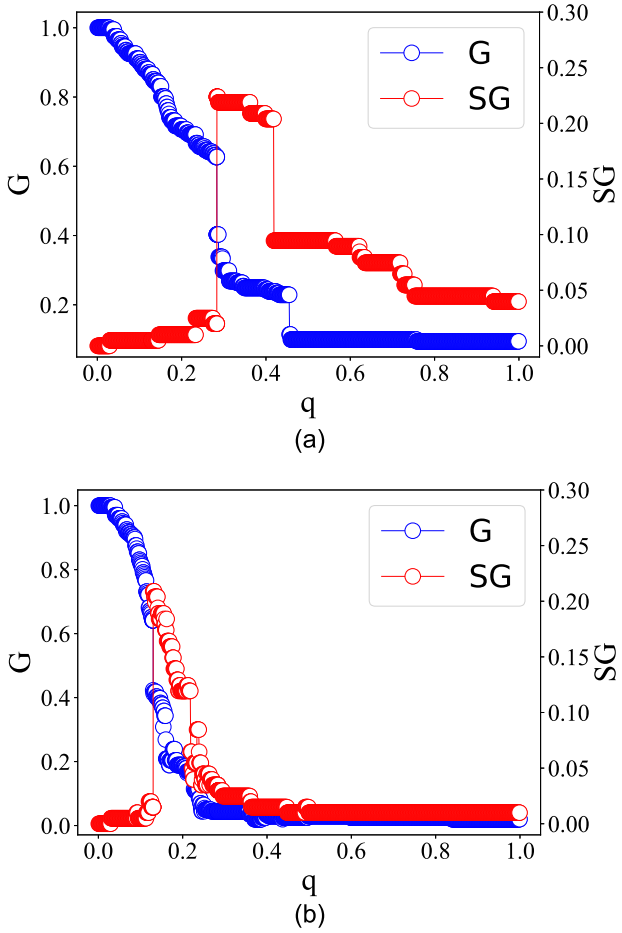

FIG. 11. Results of improving the bottleneck detected by RTP under external flow. (a) G and SG of TP. The critical value $q_c^{TP} = 0.2834$. (b) G and SG of RTP. The critical value $q_c^{RTP} = 0.1299$.

Published under an exclusive license by AIP Publishing

The volume of the bottlenecks is improved by increasing the lane number m_{ij} in Eq. (9). G and SG after improving the bottleneck detected by RTP are shown in Fig. 11. After improvement, the critical value of RTP q_c^{RTP} is increased from 0.1156 to 0.1299, almost recovered to 0.1329 when the external flow is not considered. The conditions of TP remain the same. While improving the bottlenecks identified by TP, q_c of RTP is still 0.1156.

It is worth noting that G of RTP has a surprisingly second increase caused by a new edge removed before the improvement of the bottleneck. Removing more edges improves the overall network connectivity, which is also a Braess' paradox[46] to some extent.

IV. CONCLUSION

The transition between isolated local flows and global flows helps to understand the intrinsic characteristics of traffic dynamics. However, in analyzing static networks, the mechanism of load redistribution is neglected, and the phenomenon of cascading failures is challenging to study.

In this paper, we propose a framework of RTP to fill this gap, which generates trips from origins to destinations, assigns loads to road networks via shortest paths, converts loads to velocities, and removes edges based on velocity ratios. The combination of TP and load redistribution captures the dynamics of the cascading failure, finds bottlenecks during phase transitions, and verifies the bottleneck improvement. In specific, we consider the impact of external flow on network performance and find the main influencing regions. The bottlenecks found through the cascading process are enhanced to counteract the impact of external networks to a large extent.

Using primary demographic data and network topology, we evolve urban commuting and topological improvements in this framework, providing a reference for congestion propagation of traffic networks. We provide a trip proportionality coefficient and an external traffic coefficient to enable further exploration of the traffic relationships. Since static demographic data cannot fully describe the directional flow of human behavior in urban commuting, we will further explore the combination of human behavior dynamics.

ACKNOWLEDGMENTS

We wish to acknowledge support of the National Natural Science Foundation of China (NNSFC) (Grant Nos. 11875133, 12147101, and 11075057) and the Science and Technology Commission of Shanghai Municipality (Grant No. 22JC1402500).

AUTHOR DECLARATIONS

Conflict of Interest

The authors have no conflicts to disclose.

Author Contributions

Zhuoran Chen: Conceptualization (equal); Data curation (equal); Formal analysis (equal); Investigation (equal); Methodology (equal); Software (equal); Validation (equal); Visualization (equal); Writing – original draft (equal); Writing – review & editing (equal). **Chao Yang:** Formal analysis (equal); Software (equal); Validation (equal); Visualization (equal); Writing – review & editing (equal). **Jiang-Hai Qian:** Conceptualization (equal); Methodology (equal); Writing – review & editing (equal). **Dingding Han:** Conceptualization (equal); Funding acquisition (equal); Methodology (equal); Writing – review & editing (equal). **Yu-Gang Ma:** Conceptualization (equal); Funding acquisition (equal); Methodology (equal); Writing – review & editing (equal).

DATA AVAILABILITY

The data that support the findings of this study are available from the corresponding authors upon reasonable request.

REFERENCES

[1]C. Fang, Y. Chu, H. Fu, and Y. Fang, "On the resilience assessment of complementary transportation networks under natural hazards," Transp. Res. D: Transp. Environ. **109**, 103331 (2022).
[2]Y. Abebe, G. Kabir, and S. Tesfamariam, "Assessing urban areas vulnerability to pluvial flooding using GIS applications and Bayesian belief network model," J. Cleaner Prod. **174**, 1629–1641 (2018).
[3]I. Stamos, E. Mitsakis, J. M. Salanova, and G. Aifadopoulou, "Impact assessment of extreme weather events on transport networks: A data-driven approach," Transp. Res. D: Transp. Environ. **34**, 168–178 (2015).
[4]M. A. Esfeh, L. Kattan, W. H. Lam, M. Salari, and R. A. Esfe, "Road network vulnerability analysis considering the probability and consequence of disruptive events: A spatiotemporal incident impact approach," Transp. Res. C: Emerg. Technol. **136**, 103549 (2022).
[5]A. A. Ganin, A. C. Mersky, A. S. Jin, M. Kitsak, J. M. Keisler, and I. Linkov, "Resilience in intelligent transportation systems (ITS)," Transp. Res. C: Emerg. Technol. **100**, 318–329 (2019).
[6]T. Yamada, "Generalizing the probability of reaching a destination in case of route blockage," Phys. A: Stat. Mech. Appl. **607**, 128163 (2022).
[7]S. Chen, H. Fu, N. Wu, Y. Wang, and Y. Qiao, "Passenger-oriented traffic management integrating perimeter control and regional bus service frequency setting using 3D-pMFD," Transp. Res. C: Emerg. Technol. **135**, 103529 (2022).
[8]H. Hamedmoghadam, N. Zheng, D. Li, and H. L. Vu, "Percolation-based dynamic perimeter control for mitigating congestion propagation in urban road networks," Transp. Res. C: Emerg. Technol. **145**, 103922 (2022).
[9]S. Gao, D. Li, N. Zheng, R. Hu, and Z. She, "Resilient perimeter control for hypercongested two-region networks with MFD dynamics," Transport. Res. B: Methods **156**, 50–75 (2022).
[10]Z. Chen and D. Han, "Dynamics of cyber-physical systems for intelligent transportations," in *Intelligent Equipment, Robots, and Vehicles* (Springer, 2021), pp. 511–520.
[11]K. Jin, W. Wang, X. Li, X. Hua, S. Chen, and S. Qin, "Identifying the critical road combination in urban roads network under multiple disruption scenarios," Phys. A: Stat. Mech. Appl. **607**, 128192 (2022).
[12]C. Li, W. Yue, G. Mao, and Z. Xu, "Congestion propagation based bottleneck identification in urban road networks," IEEE Trans. Veh. Technol. **69**, 4827–4841 (2020).
[13]A. Bonasera, M. Bruno, C. O. Dorso, and P. F. Mastinu, "Critical phenomena in nuclear fragmentation," Riv. Nuovo Cimento **23**, 1–101 (2000).
[14]Y. G. Ma, J. B. Natowitz, R. Wada, K. Hagel, J. Wang, T. Keutgen, Z. Majka, M. Murray, L. Qin, P. Smith, R. Alfaro *et al.*, "Critical behavior in light nuclear systems: Experimental aspects," Phys. Rev. C **71**, 054606 (2005).
[15]A. Bunde and S. Havlin, *Fractals and Disordered Systems* (Springer Science & Business Media, 2012).
[16]D. Stauffer and A. Aharony, *Introduction to Percolation Theory* (Taylor & Francis, 2018).
[17]F. Radicchi, "Percolation in real interdependent networks," Nat. Phys. **11**, 597–602 (2015).
[18]Z. Wang, M. Tang, S. Cai, Y. Liu, J. Zhou, and D. Han, "Self-awareness control effect of cooperative epidemics on complex networks," Chaos **29**, 053123 (2019).

Published under an exclusive license by AIP Publishing

[19]X. Li, X. Zhang, C. Zhao, and X. Duan, "Identification of multiple influential spreaders on networks by percolation under the SIR model," Chaos **31**, 051104 (2021).
[20]G. Dong, N. Wang, F. Wang, T. Qing, Y. Liu, and A. L. Vilela, "Network resilience of non-hub nodes failure under memory and non-memory based attacks with limited information," Chaos **32**, 063110 (2022).
[21]Z. Guo, Y. Wang, J. Zhong, C. Fu, Y. Sun, J. Li, Z. Chen, and G. Wen, "Effect of load-capacity heterogeneity on cascading overloads in networks," Chaos **31**, 123104 (2021).
[22]X. Hu, Y. Wang, H. Wang, and Y. Shi, "Hierarchical structure of the central areas of megacities based on the percolation theory—The example of Lujiazui, Shanghai," Sustainability **14**, 9981 (2022).
[23]C. Yang and Z. Chen, "Percolation on multi-layer network with joint storage and processing capacities," in *2021 13th International Conference on Computer Modeling and Simulation* (ACM, 2021), pp. 114–120; available at https://dl.acm.org/doi/abs/10.1145/3474963.3474979.
[24]C. Fan, X. Jiang, and A. Mostafavi, "A network percolation-based contagion model of flood propagation and recession in urban road networks," Sci. Rep. **10**, 1–12 (2020).
[25]Y. Shang, "Feature-enriched core percolation in multiplex networks," Phys. Rev. E **106**, 054314 (2022).
[26]D. Li, B. Fu, Y. Wang, G. Lu, Y. Berezin, H. E. Stanley, and S. Havlin, "Percolation transition in dynamical traffic network with evolving critical bottlenecks," Proc. Natl. Acad. Sci. U.S.A. **112**, 669–672 (2015).
[27]M. Saberi, H. Hamedmoghadam, M. Ashfaq, S. A. Hosseini, Z. Gu, S. Shafiei, D. J. Nair, V. Dixit, L. Gardner, S. T. Waller, and M. C. González, "A simple contagion process describes spreading of traffic jams in urban networks," Nat. Commun. **11**, 1–9 (2020).
[28]H. Hamedmoghadam, M. Jalili, H. L. Vu, and L. Stone, "Percolation of heterogeneous flows uncovers the bottlenecks of infrastructure networks," Nat. Commun. **12**, 1–10 (2021).
[29]G. Zeng, D. Li, S. Guo, L. Gao, Z. Gao, H. E. Stanley, and S. Havlin, "Switch between critical percolation modes in city traffic dynamics," Proc. Natl. Acad. Sci. U.S.A. **116**, 23–28 (2019).
[30]A. E. Motter and Y.-C. Lai, "Cascade-based attacks on complex networks," Phys. Rev. E **66**, 065102 (2002).
[31]A. E. Motter, "Cascade control and defense in complex networks," Phys. Rev. Lett. **93**, 098701 (2004).
[32]P. Crucitti, V. Latora, and M. Marchiori, "Model for cascading failures in complex networks," Phys. Rev. E **69**, 045104 (2004).
[33]R. Burkholz and F. Schweitzer, "Framework for cascade size calculations on random networks," Phys. Rev. E **97**, 042312 (2018).
[34]A. A. Ganin, M. Kitsak, D. Marchese, J. M. Keisler, T. Seager, and I. Linkov, "Resilience and efficiency in transportation networks," Sci. Adv. **3**, e1701079 (2017).
[35]F. Simini, M. C. González, A. Maritan, and A.-L. Barabási, "A universal model for mobility and migration patterns," Nature **484**, 96–100 (2012).
[36]WorldPop and C. U. Center for International Earth Science Information Network (CIESIN), "Global high resolution population denominators project" (2018).
[37]G. Voronoi, "Nouvelles applications des paramètres continus à la théorie des formes quadratiques. deuxième mémoire. recherches sur les parallélloèdres primitifs," J. Reine Angew. Math. **1908**, 198–287 (1908).
[38]G. K. Zipf, "The P_1P_2/D hypothesis: On the intercity movement of persons," Am. Sociol. Rev. **11**, 677–686 (1946).
[39]W.-S. Jung, F. Wang, and H. E. Stanley, "Gravity model in the Korean highway," EPL (Europhys. Lett.) **81**, 48005 (2008).
[40]J. de Dios Ortúzar and L. G. Willumsen, *Modelling Transport* (John Wiley & Sons, 2011).
[41]Y. He, C. Zhao, and A. Zeng, "Ranking locations in a city via the collective home-work relations in human mobility data," Phys. A: Stat. Mech. Appl. **608**, 128283 (2022).
[42]C. F. Daganzo, "The cell transmission model: A dynamic representation of highway traffic consistent with the hydrodynamic theory," Transport. Res. B: Meth. **28**, 269–287 (1994).
[43]M. Haklay and P. Weber, "Openstreetmap: User-generated street maps," IEEE Pervasive Comput. **7**, 12–18 (2008).
[44]G. Boeing, "Osmnx: New methods for acquiring, constructing, analyzing, and visualizing complex street networks," Comput. Environ. Urban Syst. **65**, 126–139 (2017).
[45]Baidu, "Traffic API" (2018).
[46]D. Braess, "Über ein paradoxon aus der verkehrsplanung," Unternehmensforschung **12**, 258–268 (1968).

Published under an exclusive license by AIP Publishing